
MANIFOLD ATTACK

Khanh-Hung Tran
Institut LIST, CEA
Université Paris-Saclay
Gif-sur-Yvette, 91191
khanh-hung.tran@cea.fr

Fred-Maurice Ngole-Mboula
Institut LIST, CEA
Université Paris-Saclay
Gif-sur-Yvette, 91191
fred-maurice.ngole-mboula@cea.fr

Jean-Luc Starck
Astrophysics Department, CEA
Université Paris-Saclay
Gif-sur-Yvette, 91191
jean-luc.starck@cea.fr

ABSTRACT

Machine Learning in general and Deep Learning in particular has gained much interest in the recent decade and has shown significant performance improvements for many Computer Vision or Natural Language Processing tasks. In order to deal with databases which have just a small amount of training samples or to deal with models which have large amount of parameters, the regularization is indispensable. In this paper, we enforce the manifold preservation (manifold learning) from the original data into latent presentation by using “manifold attack”. The later is inspired in a fashion of adversarial learning : finding virtual points that distort mostly the manifold preservation then using these points as supplementary samples to train the model. We show that our approach of regularization provides improvements for the accuracy rate and for the robustness to adversarial examples. Several implementations of our work can be found in <https://github.com/ktran1/Manifold-attack>.

1 Introduction

Deep Learning (DL) [1] has been first introduced by Alexey Ivakhnenko (1967), then its derivative Convolutional Neural Networks [2] (1980) has been introduced by Fukushima. Over the years, it was improved and refined in by Yann LeCun [3] (1998). Up to now, deep neural networks trained upon large labeled data sets have yield groundbreaking performances at various classification tasks namely in computer vision and speech recognition [4, 5, 6, 7, 8]. Training deep neural networks involves different regularization procedures which are essential, especially when only a few labeled data are available. We present three of those techniques hereafter.

First of all, data augmentation is a regularization technique through the data. It uses either transformations such as adding noise, translation or generative models, *etc*, to get more training samples. Mix-up [9], CutMix [10] can be also classed as data augmentation.

Secondly, the regularization can be performed through the model. The first strategy targets the parameters of the model. In this category, we find methods such as Dropout [11], Drop Block[12], Batch Normalization [13], Instance Normalization [14], Layer Normalization [15], Group Normalization [16]... Several models have become standard such as AlexNet, VGG, GoogleNet and ResNet. The other strategy consists in adding a regularization loss to the objective function. This regularization can simply be a square loss of trainable parameters of model (Weight decay [17]) or, in the most cases, an auxiliary loss for a task that differs from the main one. Optimizing the model for both the main loss and auxiliary loss might help it to learn more relevant features, therefore improving its performance. The auxiliary loss can contain unlabelled samples, turning the original problem into a semi-supervised learning task. The auxiliary can tackle different tasks like, for instance, preserving properties of original data into a latent representation or classifying samples in a self-supervised manner, where annotations are generated automatically [18].

Finally, the regularization might be done to the optimization procedure itself like Early Stopping [19, 20], Adam [21], Cosine Annealing [22]. A taxonomy of regularization and an evaluation of model effective capacity can be found respectively in [23, 24].

We develop a regularization based on the mechanism called Virtual Adversarial Training (VAT) [25], which is the data augmentation combined with adversarial learning. Our approach differs from this work in the generation of virtual

points: a virtual point is created by linear combination of several data samples, as opposed to one created by adding noise to a data sample. In more details, given a data sample, adding adversarial noise means that we look for an adversarial sample only in the locality of this sample. On the other hand, our approach allows us to look for adversarial samples further in the manifold of data.

The outline of the paper is as follows. In section 2, we revisit some classical manifold learning methods. In section 3, we present manifold attack, which introduces the adversarial learning into classical manifold learning. Several settings for manifold attack can be found in section 4. The numerical experiments are presented and discussed in section 5. We show that our proposed algorithm helps to improve tasks such as manifold learning (for data visualization), classification and robustness to adversarial examples. Our conclusions and perspectives are presented in section 6.

2 Manifold learning

Given data set $\mathcal{X} = \{\mathbf{x}_1, \dots, \mathbf{x}_N\}$, $\mathbf{x}_i \in \mathbb{R}^n$ and its embedded set $\mathcal{A} = \{\mathbf{a}_1, \dots, \mathbf{a}_N\}$, $\mathbf{a}_i \in \mathbb{R}^d$, where \mathbf{a}_i is the embedded representation of \mathbf{x}_i , we note

$$\mathcal{L}_e(\mathbf{a}_i, \mathcal{A}_i^c),$$

the embedding loss from a data point (or data sample) versus all resting data points, where \mathcal{A}_i^c is the complement of $\{\mathbf{a}_i\}$ in \mathcal{A} . We present some popular embedding losses hereafter.

Multidimensional scaling (MDS) [26] :

$$\mathcal{L}_e(\mathbf{a}_i, \mathcal{A}_i^c) = \sum_{\mathbf{a}_j \in \mathcal{A}_i^c} (d_a(\mathbf{a}_i, \mathbf{a}_j) - d_x(\mathbf{x}_i, \mathbf{x}_j))^2,$$

where $d_a()$ and $d_x()$ are metrics for dissimilarity measure. By default, they are both Euclidean distances.

Laplacian eigenmaps (LE) [27] :

$$\mathcal{L}_e(\mathbf{a}_i, \mathcal{A}_i^c) = \sum_{\mathbf{a}_j \in \mathcal{A}_i^c} d_x(\mathbf{x}_i, \mathbf{x}_j) d_a(\mathbf{a}_i, \mathbf{a}_j),$$

where $d_x()$ is a metric for similarity measure, by default $d_x(\mathbf{x}_i, \mathbf{x}_j) = \exp\left(\frac{-\|\mathbf{x}_i - \mathbf{x}_j\|_2}{2\sigma_i^2}\right)$ and $d_a()$ is a metric for dissimilarity measure, by default $d_a(\mathbf{a}_i, \mathbf{a}_j) = \|\mathbf{a}_i - \mathbf{a}_j\|_2^2$.

Contrastive loss :

$$\mathcal{L}_e(\mathbf{a}_i, \mathcal{A}_i^c) = \sum_{\mathbf{a}_j \in \mathcal{A}_i^c} \left(d_x(\mathbf{x}_i, \mathbf{x}_j) d_a(\mathbf{a}_i, \mathbf{a}_j) + (1 - d_x(\mathbf{x}_i, \mathbf{x}_j)) \max(0, \tau - d_a(\mathbf{a}_i, \mathbf{a}_j)) \right),$$

where $d_x(\mathbf{x}_i, \mathbf{x}_j)$ is a discrete similarity metric which is equal to 1 if \mathbf{x}_j is in the neighborhood (Euclidean metric by default) of \mathbf{x}_i and 0 if not. $d_a()$ is a metric for dissimilarity measure, by default $d_a(\mathbf{a}_i, \mathbf{a}_j) = \|\mathbf{a}_i - \mathbf{a}_j\|_2^2$.

Locally Linear Embedding (LLE) [28]:

$$\mathcal{L}_e(\mathbf{a}_i, \mathcal{A}_i^c) = \left\| \mathbf{a}_i - \sum_{\mathbf{a}_j \in \mathcal{A}_i^c} \lambda_{ij} \mathbf{a}_j \right\|_2^2,$$

where λ_{ij} are determined by optimizing the following problem :

$$\begin{aligned} & \min \left\| \mathbf{x}_i - \sum_j \lambda_{ij} \mathbf{x}_j \right\|_2^2, \\ & \text{subject to : } \begin{cases} \sum_j \lambda_{ij} = 1, & \text{if } \mathbf{x}_j \in \text{knn}(\mathbf{x}_i), \\ \lambda_{ij} = 0 & \text{if not.} \end{cases} \end{aligned}$$

where $\text{knn}(\mathbf{x}_i)$ means the set that contains k nearest neighbors of \mathbf{x}_i .

Stochastic Neighbor Embedding (SNE) [29]:

$$\mathcal{L}_e(\mathbf{a}_i, \mathcal{A}_i^c) = \sum_{\mathbf{a}_j \in \mathcal{A}_i^c} P_{ij} \log \frac{P_{ij}}{Q_{ij}},$$

where $P_{ij} = \frac{d_x(\mathbf{x}_i, \mathbf{x}_j)}{\sum_{k \neq i} d_x(\mathbf{x}_i, \mathbf{x}_k)}$ and $Q_{ij} = \frac{d_a(\mathbf{a}_i, \mathbf{a}_j)}{\sum_{k \neq i} d_a(\mathbf{a}_i, \mathbf{a}_k)}$, d_x and d_a are both similarity metric.

Finally, the embedding problem is defined as:

$$\min_{\mathcal{A}} \mathcal{L}_t = \min_{\mathcal{A}} \sum_i \mathcal{L}_e(\mathbf{a}_i, \mathcal{A}_i^c)$$

Note that, for LE and LLE, some supplement constrains are required to avoid a trivial solution (all embedded points are collapsed into only one point). There are two types of manifold learning techniques: with mapping model such as SNE and without mapping model such as LE and LLE. A mapping model here is a function $g()$ with trainable parameters that maps a sample \mathbf{x} to its embedded representation \mathbf{a} as $\mathbf{a} = g(\mathbf{x})$. For manifold learning with model, the loss function \mathcal{L}_t is optimized by considering trainable parameters of $g()$ as variables and the model $g()$ advantageously provides the embedding of out-of-samples points. On the other hand, for manifold learning without model, \mathcal{L}_t is optimized by considering directly embedded representation \mathcal{A} as the variable. To embed an out of sample point, a new optimization has to be performed. In our work, we consider only manifold learning with model since the manifold attack, which is presented in the next section, requires an explicit relation between the sample and its embedded representation.

3 Manifold attack

As in the classification task, the over-fitting problem can also happen in the manifold learning task: a sample which is not in training set can be mapped to the wrong position in the embedded space. There is this famous example which shows that a small amount of additive noise can get a learnt model to misclassify a panda by a gibbon [30]. This means that the model, in this case, does not guarantee neighboring samples in the original space have similar embedded representations.

We start with our definition for virtual point (virtual sample) and attack point. A virtual point is a supplement sample (not data sample), which is crafted by user and is believed in the manifold of data. An example for virtual point is a data point with a random noise. An attack point is a virtual point that aims to distort the model. An example for attack point is a data point with an adversarial noise.

In the fashion of virtual adversarial training, we create and find attack points that distort the embedded manifold, *i.e.*, to maximize the loss function \mathcal{L}_t while fixing the current model $g()$, then we update the model $g()$ to minimize this loss function while fixing the attack points. First of all, we define our virtual point and its feasible zone. Let consider p anchor points $\mathbf{z}_1, \mathbf{z}_2, \dots, \mathbf{z}_p \in \mathbb{R}^n$, a virtual point $\tilde{\mathbf{x}} \in \mathbb{R}^n$ is defined as :

$$\begin{aligned} \tilde{\mathbf{x}} &= \gamma_1 \mathbf{z}_1 + \gamma_2 \mathbf{z}_2 + \dots + \gamma_p \mathbf{z}_p, \\ \text{subject to : } &\gamma_1, \gamma_2, \dots, \gamma_p \geq 0, \\ &\gamma_1 + \gamma_2 + \dots + \gamma_p = 1. \end{aligned} \tag{1}$$

The anchor points \mathbf{z}_i define a region or feasible zone in which the virtual point $\tilde{\mathbf{x}}$ must be located and $\gamma = [\gamma_1, \gamma_2, \dots, \gamma_p]$ is the coordinate of $\tilde{\mathbf{x}}$. The anchor points, in general, are sampled from data \mathcal{X} with different strategies. The strategy for setting anchor points, is defined according to a user provided rule (see section 4, for several examples). The fig. 1 shows an example for setting of anchor points and relations between points.

The algorithm 1 describes an individual manifold attack from a virtual point. Beside the embedding loss created by an embedded data point $g(\mathbf{x}_i)$ versus its counterparts :

$$\mathcal{L}_e(\mathbf{a}_i, \mathcal{A}_i^c) = \mathcal{L}_e(g(\mathbf{x}_i), \{g(\mathbf{x}_1), \dots, g(\mathbf{x}_N)\} \setminus \{g(\mathbf{x}_i)\})$$

as mentioned in 2, we construct, in addition, the embedding loss created by an embedded virtual point versus embedded data points :

$$\mathcal{L}_e(\tilde{\mathbf{a}}, \mathcal{A}) = \mathcal{L}_e(g(\tilde{\mathbf{x}}), \{g(\mathbf{x}_1), \dots, g(\mathbf{x}_N)\})$$

where $\tilde{\mathbf{a}} = g(\tilde{\mathbf{x}})$ is embedded representation of virtual point. The virtual point $\tilde{\mathbf{x}}$ is initialized by γ then it becomes attack point, in order to give a local maximum of \mathcal{L}_e .

We have that the number of virtual points depends on the number of sets of anchor points. A set of anchor points can generate more than one virtual point by using different initialization of γ , to find different local maximums. Combining the embedding losses from embedded data points versus their counterpart data points and the ones from embedded virtual points versus embedded data points, we expect to regularize better the model $g()$.

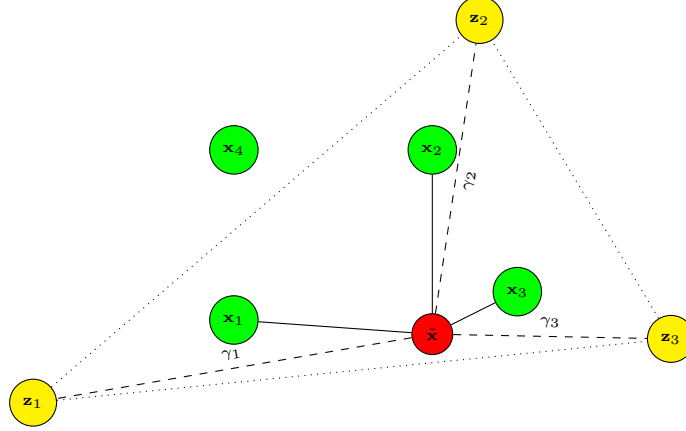


Figure 1: An illustration about virtual point, anchor points. The three anchor points ($i \in \{1, 2, 3\}$) are created as $\mathbf{z}_i = \mu([\mathbf{x}_1, \mathbf{x}_2, \mathbf{x}_3]) + s(\mathbf{x}_i - \mu([\mathbf{x}_1, \mathbf{x}_2, \mathbf{x}_3]))$, where $\mu([\mathbf{x}_1, \mathbf{x}_2, \mathbf{x}_3]) = \frac{\mathbf{x}_1 + \mathbf{x}_2 + \mathbf{x}_3}{3}$. The dotted lines represent the feasible zone defined by anchor points \mathbf{z}_i , means that the virtual point $\tilde{\mathbf{x}}$ is always inside this zone. The later is controlled by the parameter s that allows to explore outside ($s > 1$) or to restrain strictly inside ($0 > s > 1$) of the polytope defined by $[\mathbf{x}_1, \mathbf{x}_2, \mathbf{x}_3]$. The dashed lines represent the coordinates γ of $\tilde{\mathbf{x}}$. The solid lines represent the interaction of $\tilde{\mathbf{x}}$ versus data points to create the embedding loss which is $\mathcal{L}_e(g(\tilde{\mathbf{x}}), \{g(\mathbf{x}_1), g(\mathbf{x}_2), g(\mathbf{x}_3)\})$ in this case.

Algorithm 1 Individual manifold attack

Require: Anchor points $\{\mathbf{z}_1, \dots, \mathbf{z}_p\}$, data points $\{\mathbf{x}_1, \dots, \mathbf{x}_N\}$, embedding loss $\mathcal{L}_e(\cdot)$, model $g(\cdot)$, ξ, n_iters .

1: **initialize** : $\gamma \in \mathbb{R}^p, \gamma = [\gamma_1, \dots, \gamma_p]$ for constraints in eq. (1)

2: $\tilde{\mathbf{x}} = \gamma_1 \mathbf{z}_1 + \gamma_2 \mathbf{z}_2 + \dots + \gamma_p \mathbf{z}_p$

3: **for** $i = 1$ **to** n_iters **do**

4: $L = \mathcal{L}_e(g(\tilde{\mathbf{x}}), \{g(\mathbf{x}_1), \dots, g(\mathbf{x}_N)\})$

5: $\gamma \leftarrow \gamma + \xi \nabla_{\gamma} L(\tilde{\mathbf{x}})$

6: $\gamma \leftarrow \Pi_{ps}(\gamma)$

7: $\tilde{\mathbf{x}} = \gamma_1 \mathbf{z}_1 + \gamma_2 \mathbf{z}_2 + \dots + \gamma_p \mathbf{z}_p$

8: **end for**

9: **Output** : $\tilde{\mathbf{x}}$

Finding virtual point $\tilde{\mathbf{x}}$ is equivalent to finding γ with constrains as in eq. (1). The later is performed by a gradient-based method. After updating γ by gradient, a projection is required to ensure the constraints for γ . This projection Π_{ps} is defined as :

$$\begin{aligned} & \min_{\gamma \in \mathbb{R}^p} \frac{1}{2} \|\kappa - \gamma\|_2^2, \\ & \text{subject to : } \gamma_1, \gamma_2, \dots, \gamma_p \geq 0, \\ & \gamma_1 + \gamma_2 + \dots + \gamma_p = c, (c > 0). \end{aligned} \tag{2}$$

This convex problem with constraints can be solved quickly by a simple sequential projection that alternates between sum constraint and positive constraint (algorithm 2). The demonstration can be inspired by the Lagrange multiplier method. This algorithm can be extended for executing in parallel multiple virtual points at the same time ($\gamma \in \mathbb{R}^{M \times p}$, where M is the number of virtual points). An implementation of algorithm 2 can be found in section 6.

In algorithm 1, there are only interactions from a virtual point versus data points. We extend this case into the general manifold attack (algorithm 3), in order to take into account all interactions between points, which can be both data points or virtual points. From now, the role of virtual point is exactly as supplement data point. We denote \mathcal{B} as a set that contains all embedded points (both virtual and data). \mathcal{B}_s is a random subset of \mathcal{B} , in order to perform optimization by batch. In each step, only virtual points of batch are learned to distort the manifold by maximizing the batch loss L . The effect between virtual points and data points can be controlled via the subset \mathcal{B}_s , by tuning the ratio between the number of virtual points and the number of data points (removing a number of virtual points).

Algorithm 2 Projection for positive and sum constraint Π_{ps}

Require: $\kappa \in \mathbb{R}^p$, $c = 1$ (by default).

- 1: $\delta = (c - \sum_{i=1}^p \kappa_i) / p$
 - 2: $\gamma_i \leftarrow \gamma_i + \delta, \forall i = 1, \dots, p$
 - 3: **while** $\exists i \in \{1, \dots, p\} : \gamma_i < 0$ **do**
 - 4: $\mathcal{P} = \{i | \gamma_i > 0\}$ and $\mathcal{N} = \{i | \gamma_i < 0\}$
 - 5: $\gamma_i \leftarrow 0, \forall i \in \mathcal{N}$
 - 6: $\delta = (c - \sum_{i \in \mathcal{P}} \gamma_i) / |\mathcal{P}|$
 - 7: $\gamma_i \leftarrow \gamma_i + \delta, \forall i \in \mathcal{P}$
 - 8: **end while**
 - 9: **Output :** $\gamma = [\gamma_1, \gamma_2, \dots, \gamma_p]$
-

Algorithm 3 Manifold attack

Require: Data points $\{\mathbf{x}_1, \dots, \mathbf{x}_N\}$, embedding loss $\mathcal{L}_e()$, model $g()$, ξ , n_iters , an anchor rule.

- 1: **initialize :** $g()$
 - 2: Create M sets of anchor points $\{\mathbf{z}_1^k, \dots, \mathbf{z}_p^k\}, \forall k = 1, \dots, M$ by the anchor rule
 - 3: **for** $epoch = 1$ **to** n_epoch **do**
 - 4: Initialize $\gamma^k \in \mathbb{R}^p$ for constraints in eq. (1)
 - 5: $\tilde{\mathbf{x}}^k = \gamma_1^k \mathbf{z}_1^k + \gamma_2^k \mathbf{z}_2^k + \dots + \gamma_p^k \mathbf{z}_p^k, \forall k = 1, \dots, M$
 - 6: Set $\mathcal{B} = \{g(\tilde{\mathbf{x}}^1), \dots, g(\tilde{\mathbf{x}}^M)\} \cap \{g(\mathbf{x}_1), \dots, g(\mathbf{x}_N)\}$ and divide it into subsets \mathcal{B}_s
 - 7: **for each** \mathcal{B}_s **do**
 - 8: $L = \sum_{\mathbf{a} \in \mathcal{B}_s} \mathcal{L}_e(\mathbf{a}, \mathcal{B}_s \setminus \{\mathbf{a}\})$
 - 9: Update $\{\tilde{\mathbf{x}}^i | g(\tilde{\mathbf{x}}^i) \in \mathcal{B}_s\}$ to maximize L by algorithm 4
 - 10: Update $g()$ to minimize L
 - 11: **end for**
 - 12: **end for**
 - 13: **Output :** $g()$
-

algorithm 4 represents the update step for multiple virtual points. The gradient update for γ is the simplest version by default and we can replace it by the other one in gradient-based family. Since the attack stage is executed a lot of times (alternatively with updating model $g()$), we recommend to use n_iter that approximates to less than 5 iterations. In our work, the attack is based on gradient-based method, therefore the embedding loss \mathcal{L}_e need to be continuous with respect to γ . Nevertheless, in manifold learning field, there are several methods whose embedding loss is not continuous, for example, LLE in section 2, the embedding loss takes into account the k nearest neighbors of a point. Imagine that after a gradient update step in manifold attack, a virtual point changes several neighbors among its actual k nearest neighbors, then the embedding loss for this virtual point takes into account new neighbors, which make it discontinuous. To circumvent this problem, we try to keep the loss embedding continuous by several strategies :

- By the anchor rule. We set anchor points in order that a virtual point, which is inside the zone defined by anchor points, does not change its k nearest neighbors.
- By reducing the gradient step ξ or the number of iterations n_iter , which restrains the movement of virtual point.
- By selecting a small subset \mathcal{B}_s or removing a number of virtual points to perform the attack while fixing other virtual points.
- By updating γ only if embedding loss increases.

Moreover, for the contrastive loss in section 2, we can redefine the metric in , the metric $d_x()$ which outputs value as 0 or 1, can be replaced by $d_x(\mathbf{x}_i, \mathbf{x}_j) = \exp\left(\frac{-\|\mathbf{x}_i - \mathbf{x}_j\|_2^2}{2\sigma_i^2}\right)$ to make embedding loss continuous.

Pairwise manifold learning

For some manifold learning methods as MDS or LE, the embedding loss \mathcal{L}_e can be decomposed into the sum of elementary pairwise loss l_e :

$$\mathcal{L}_e(\mathbf{a}, \mathcal{B}) = \sum_{\mathbf{b} \in \mathcal{B}} l_e(\mathbf{a}, \mathbf{b})$$

Algorithm 4 Virtual points update

Require: m sets of anchor points $\{\mathbf{z}_1^k, \dots, \mathbf{z}_p^k\}, \gamma^k, \forall k = 1, \dots, m$, loss $L()$, ξ, n_iters .

- 1: $\tilde{\mathbf{x}}^k = \gamma_1^k \mathbf{z}_1^k + \gamma_2^k \mathbf{z}_2^k + \dots + \gamma_p^k \mathbf{z}_p^k, \forall k = 1, \dots, m$
 - 2: **for** $i = 1$ **to** n_iters **do**
 - 3: Calculate gradient ∇L (w.r.t $[\gamma^1, \dots, \gamma^m]$) of function $L(\tilde{\mathbf{x}}^1, \dots, \tilde{\mathbf{x}}^m)$
 - 4: $[\gamma^1, \dots, \gamma^m] \leftarrow [\gamma^1, \dots, \gamma^m] + \xi \nabla_{\gamma} L(\tilde{\mathbf{x}}^1, \dots, \tilde{\mathbf{x}}^m)$
 - 5: $\gamma^k \leftarrow \Pi_{ps}(\gamma^k), \forall k = 1, \dots, m$
 - 6: $\tilde{\mathbf{x}}^k = \gamma_1^k \mathbf{z}_1^k + \gamma_2^k \mathbf{z}_2^k + \dots + \gamma_p^k \mathbf{z}_p^k, \forall k = 1, \dots, m$
 - 7: **end for**
 - 8: **Output :** $\tilde{\mathbf{x}}^1, \dots, \tilde{\mathbf{x}}^m$
-

Then the batch loss L (in algorithm 3) can be modified into :

$$L = \sum_{\mathbf{a} \in \mathcal{B}_s} \mathcal{L}_e(\mathbf{a}, \mathcal{B}_s \setminus \{\mathbf{a}\}) = \sum_{\mathbf{a} \in \mathcal{B}_s} \sum_{\mathbf{b} \in \mathcal{B}_s, \mathbf{b} \neq \mathbf{a}} l_e(\mathbf{a}, \mathbf{b})$$

By this modification, L can be decomposed into three parts :

$$\begin{aligned} & \sum_{\mathbf{a} \in \mathcal{B}_s^d} \sum_{\mathbf{b} \in \mathcal{B}_s^d, \mathbf{b} \neq \mathbf{a}} l_e(\mathbf{a}, \mathbf{b}) && \text{(data-data)} \\ & \sum_{\mathbf{a} \in \mathcal{B}_s^d} \sum_{\mathbf{b} \in \mathcal{B}_s^v} l_e(\mathbf{a}, \mathbf{b}) && \text{(data-virtual)} \\ & \sum_{\mathbf{a} \in \mathcal{B}_s^v} \sum_{\mathbf{b} \in \mathcal{B}_s^v, \mathbf{b} \neq \mathbf{a}} l_e(\mathbf{a}, \mathbf{b}) && \text{(virtual-virtual),} \end{aligned}$$

where \mathcal{B}_s^d and \mathcal{B}_s^v are respectively set that contains all embedded data points and all embedded virtual points of \mathcal{B}_s .

In pairwise manifold learning, we can further control the effect between virtual points and data points, not only by tuning the ratio between the number of virtual points and the number of data points in \mathcal{B}_s , but also by attaching a weight for each of three above parts. The attached weights favor the most for the case data-data, then data-virtual and virtual-virtual. The effect between virtual points and data points is important because virtual points are assumed to be in the manifold of data at the beginning, but they can go out the manifold of data in the attack stage (As in the case Random anchors in section 4). The elementary pairwise loss l_e for each part is not required to be the same, for example, we can use l_e in MDS for data-data and l_e in LE for data-virtual...

4 Settings of anchor points and initialization for virtual points

In this section, we provide two settings (or rules) of anchor points with its corresponding initialization. This setting need to be taken carefully to guarantee that virtual points are always in the manifold of data in attack stage.

Neighbor anchors

: The first anchor point \mathbf{z}_1 is taken randomly from \mathcal{X} , then the next $(p - 1)$ anchor points $\mathbf{z}_2, \dots, \mathbf{z}_p$ are taken as $(p - 1)$ nearest neighbor points of \mathbf{z}_1 in \mathcal{X} (Euclidean metric by default). Here, we assume that a zone defined by a data point and its neighbors is always in the manifold of data \mathcal{X} . The number of anchors p need to be small compared to the number of data points N . The initialization for virtual point can be set by taking $\gamma_i \sim \mathcal{U}(0, 1), \forall i = 1, \dots, p$ then normalize to have $\sum_{i=1}^p \gamma_i = 1$.

Random anchors

: The second setting is inspired based on mix-up method [9]. p anchors are taken randomly from \mathcal{X} and we take $\gamma \sim \text{Dirichlet}(\alpha_1, \dots, \alpha_p)$. If $\alpha_i \ll 1, \forall i = 1, \dots, p$, the Dirichlet distribution returns γ where $\gamma_i \geq 0, \sum_{i=1}^p \gamma_i = 1$ and especially, with a strong probability, there is a coefficient γ_k much greater than other ones. The later means that virtual points are more probably in the neighborhood of a data point. Since the manifold attack try to find only local maximum by gradient-based method, if ξ and n_iters are both small, we expect that virtual points in the attack stage

do not move too far from their initiated position, then they are always in the manifold of data. Note that, in the case $\alpha_i = 1, \forall i = 1, \dots, p$, the Dirichlet distribution become the Uniform distribution.

To ensure that there is always a coefficient γ_k which is much greater than other ones, we can adjust one more constraint for γ , as $\gamma_k \geq \tau$, and by taking τ close to 1. The constraints in eq. (1) become :

$$\begin{aligned} \gamma_1, \gamma_2, \dots, \gamma_p &\geq 0, \\ \gamma_1 + \gamma_2 + \dots + \gamma_p &= 1, \\ \gamma_k &\geq \tau, (\tau < 1). \end{aligned}$$

Then the projection in algorithm 2 need to be slightly modified to adapt this new constraint. We define the projection $\gamma = \Pi'_{ps}(\kappa)$ as follow:

$$\begin{aligned} \kappa' &\leftarrow \kappa \\ \kappa'_k &\leftarrow \kappa'_k - \tau \\ \gamma &\leftarrow \Pi_{ps}(\kappa', c = 1 - \tau) \\ \gamma_k &\leftarrow \gamma_k + \tau \end{aligned} \tag{3}$$

5 Numerical experiments

We organize this section as follows. First, we show the advantage of the manifold attack for embedding the S curve data and Digit data, in the case of small amount of data. This experiment is performed with two manifold learning methods : multidimensional scaling (MDS) and Laplacian eigenmaps (LE). In the second experiment, we convert mix-up method into its attack version by adding a simple attack stage and show that the attack version is more robust against adversarial examples. The data using in this experiment is ImageNet [31]. Finally, we convert Mix Match, a semi-supervised method, into its attack version and show that the attack version helps also to improve the accuracy rate on CIFAR-10 [32] and SVHN dataset [33].

5.1 Manifold attack for embedded representation

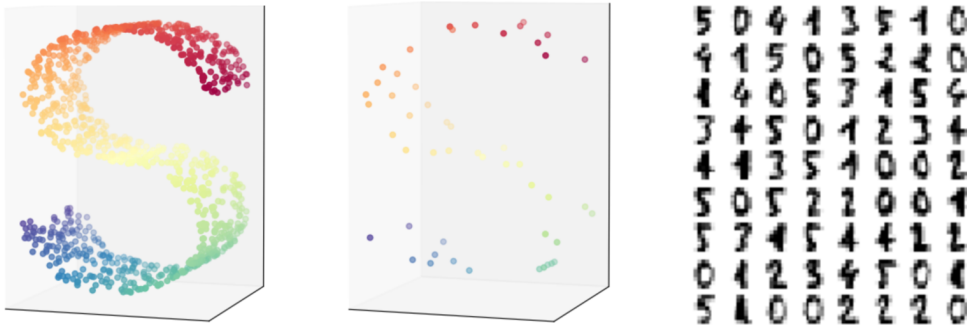


Figure 2: Left : S curve data 1000 samples. Center : S curve data 50 samples. Right : Digit data.

The S curve data and Digit data are created by the module *datasets* in *scikit-learn*. The S curve data contains $N = 1000$ samples, each sample is 3-dimensional, as showed in fig. 2. The Digit data contains $N = 1797$ samples, each sample is a 8×8 image of a digit number. We expect to embed these data into 2-dimensional embedded representation. Each data is separated into two sets : N_{tr} samples are randomly taken for training set and the N_{te} resting samples are for testing set. We denote \mathbf{x} as a sample, \mathbf{x}^{tr} as a training sample and \mathbf{x}^{te} as a testing sample. We perform four training modes, which are described in table 1.

The evaluation loss, after optimizing model $g()$, is defined as :

$$L_{ev} = \frac{1}{N_{te}} \sum_{i=1}^{N_{te}} \mathcal{L}_e(g(\mathbf{x}_i^{te}), \{g(\mathbf{x}_j^{te}) | j \neq i\})$$

Before going in the training process, we need to define the anchor rule, embedding loss \mathcal{L}_e and the model $g()$.

Anchor rule : we perform two settings of anchor points:

Mode	Description of objective function
1. REF	Manifold learning that takes into account both training and testing samples : $L_{tr} = \frac{1}{N} \sum_{i=1}^N \mathcal{L}_e(g(\mathbf{x}_i), \{g(\mathbf{x}_j) j \neq i\})$ The result of this training mode is considered as “reference” in order to compare to other training modes.
2. DD	Manifold learning that takes only training data samples : $L_{tr} = \frac{1}{N_{tr}} \sum_{i=1}^{N_{tr}} \mathcal{L}_e(g(\mathbf{x}_i^{tr}), \{g(\mathbf{x}_j^{tr}) j \neq i\})$
3. RV	Random virtual, virtual points are only randomly initialized and without attack stage (by setting $n_iters = 0$ in algorithm 4) : $L_{tr} = \frac{1}{ \mathcal{B} } \sum_{\mathbf{a}_i \in \mathcal{B}} \mathcal{L}_e(\mathbf{a}_i, \mathcal{B} \setminus \{\mathbf{a}_i\}),$ where $\mathcal{B} = \{g(\tilde{\mathbf{x}}^1), \dots, g(\tilde{\mathbf{x}}^M)\} \cap \{g(\mathbf{x}_1^{tr}), \dots, g(\mathbf{x}_{N_{tr}}^{tr})\}$.
4. MA	Manifold attack, the same objective function as the previous case, except $n_iters \neq 0$.

Table 1: Four training modes : REF (Reference), DD (Data-Data), RV (Random Virtual) and MA (Manifold Attack), and their corresponding objective function.

- *Neighbor anchors* (NA) : A set of anchor points is composed by a training point with its 4 nearest neighbors. In this case, we have $M = N_{tr}$ sets of anchor points and $p = 5$. The coefficient γ is initialized by the Uniform distribution.
- *Random anchors* (RA) : We take randomly 2 points among N_{tr} training points to create a set of anchor points. In this case, we have $M = \binom{N_{tr}}{2}$ sets of anchor points and $p = 2$. The coefficient γ is initialized by the Dirichlet distribution with $\alpha_i = 0.5, \forall i = 1, \dots, p$.

The embedding loss \mathcal{L}_e used are MDS method and LE method as described in section 2, with the metrics by default. For similarity metric $d_x()$ in LE method, we take $\sigma = 0.2$ for S curve data and $\sigma = 0.5$ for Digit data.

The model $g()$ used is a simple convolutional neural network, more details about its architecture can be found in section 6. For LE method, we impose two supplement constraints, in particular to avoid that all embedded points collapse into only one point :

$$\begin{aligned} \mathbf{E}(\mathbf{A}^{tr}) &= [\mathbf{E}(\mathbf{A}^{tr}[1, :]), \dots, \mathbf{E}(\mathbf{A}^{tr}[d, :])]^\top = \mathbf{0}_d \\ \Sigma(\mathbf{A}^{tr}, \mathbf{A}^{tr}) &= \mathbf{I}_d \end{aligned}$$

where $d = 2$ is the number of output dimensions, $\mathbf{A}^{tr} = [\mathbf{a}_1^{tr}, \dots, \mathbf{a}_{N_{tr}}^{tr}] = [g(\mathbf{x}_1^{tr}), \dots, g(\mathbf{x}_{N_{tr}}^{tr})]$. To adapt these constraints, we adjust a normalization layer at the end of model $g() : (g(\mathbf{x}) - \mathbf{E}(\mathbf{A}^{tr}))\Sigma^{-1}(\mathbf{A}^{tr}, \mathbf{A}^{tr})$, where Σ^{-1} is performed by Cholesky decomposition.

In case of a few training samples, we fix $N_{tr} = 100$ for MDS method and $N_{tr} = 50$ for LE method. The effect between virtual points and data points is controlled by the couple $\lambda = (\text{number of virtual points in } \mathcal{B}_s, \text{ number of data points in } \mathcal{B}_s)$. We set $\lambda = (2, 5)$ for MDS method and $\lambda = (5, 10)$ for LE method. The gradient step ξ is tuned from $\{0.1, 1, 10\}$ and the number of iteration is fixed at $n_iters = 1$.

Since using manifold learning with model, the initialization of model $g()$ has an important impact, especially in the case of small amount of training data, we perform five different initialization of model for each method, the mean and the standard deviation of evaluation loss L_{ev} are reported in table 2. First, we see that using random virtual points as supplement data points (RV) gives a better loss than using only data points (DD), this is evident since we use more

samples to train the model. Second, using manifold attack (MA) gives a better loss than using random virtual (RV), which shows the advantage of adversarial learning in general and our proposed approach in particular, to regularize the model.

For the S curve data, initialization by *Neighbors anchors* gives a better result compared to initialization by *Random anchors*. However, for the Digit data, initialization by *Random anchors* gives a better result. This is due to the fact that in the S curve data, *Neighbor Anchors* covers better the manifold of data than *Random Anchor*. On the other hand, in Digit data, *Neighbor Anchors* (by using Euclidean metric to determine nearest neighbors) can generate, with greater probability, a virtual point that is not in the manifold of data. This leads to a greater evaluation loss compared to *Random Anchor*.

The five embedded representations for testing sample of S curve data can be found in fig. 3 for MDS method and in fig. 4 for LE method (in section 6).

Mode / Method	S curve data		Digit data	
	MDS	LE	MDS	LE
REF	130.7 ± 24.74	0.399 ± 0.07	2015 ± 14	0.07 ± 0.002
DD	352.56 ± 119.19	1.21 ± 0.46	2409 ± 78	0.58 ± 0.07
RV (NA)	173.87 ± 9.38	0.59 ± 0.11	2395 ± 73	0.31 ± 0.03
MA (NA)	170.62 ± 5.89	0.55 ± 0.07	2362 ± 63	0.24 ± 0.03
RV (RA)	183.42 ± 18.13	0.65 ± 0.14	2342 ± 56	0.22 ± 0.03
MA (RA)	169.04 ± 5.30	0.63 ± 0.14	2331 ± 56	0.2 ± 0.02

Table 2: Evaluation loss L_{ev} of two manifold learning methods MDS and LE, in four modes : REF, DD, RV, MA and two initialization strategies : Neighbor Anchors (NA) and Random Anchors (RA).

5.2 Robustness to adversarial examples

In this subsection, we provide an attack version of supervised learning approach Mix-up [9] and study the robustness to adversarial examples. Let y_i (one hot vector) denote the label of \mathbf{x}_i , N_l denote the number of labelled samples, we recall the empirical risk minimization (ERM) for the classical supervised case:

$$L_{ERM} = \frac{1}{N_l} \sum_{i=1}^{N_l} \mathcal{L}_c(g(\mathbf{x}_i), y_i),$$

where \mathcal{L}_c is usually the Cross Entropy function. In Mix-up method, we try to generate more labelled samples, by combining linearly two random samples and their corresponding label. This linear combination is controlled by $\gamma = [\gamma_1, \gamma_2]$. We recall the objective function in Mix-up method :

$$L_{MU} = \frac{1}{N_l^2} \sum_{i=1}^{N_l} \sum_{j=1}^{N_l} \mathbb{E}_{\gamma_1} [\mathcal{L}_c(\gamma_1 \mathbf{x}_i + \gamma_2 \mathbf{x}_j, \gamma_1 y_i + \gamma_2 y_j)]$$

where: $\gamma_1 + \gamma_2 = 1$ and $\gamma_1 \sim \text{Beta}(\alpha, \alpha)$

In Mix-up attack, we add a simple attack stage after each sampling of γ from the Beta distribution, to find γ that gives the greater loss L_{MU} , before minimizing the model $g(\cdot)$. The attack stage is performed by using algorithm 4 with loss L here is a batch loss of L_{MU} . As in Mix-up, the number of anchor points p equals to 2, we can express $\gamma_2 = 1 - \gamma_1$, then we need to deal with only one variable γ_1 to maximize the batch loss L . The projection 2 for γ_1 is now just the clamping function, to make sure that γ_1 is between 0 and 1. To be in the same configuration as Mix-up, in a batch, all pairs of data samples are linearly combined by the same pair γ_1, γ_2 .

We perform four supervised training methods: ERM, Mix-up, Mix-up attack and Cut-Mix [10] on ImageNet dataset with the model ResNet-50 [6], which has about 25.7M trainable parameters. We use ImageNet downloader by [34] to download about 1000 classes and 550 each class by Uniform Resource Locator (url). However, since a lot of urls do not exist anymore, we have only 948 available classes that each class has 400 labelled training samples and 50 testing samples to evaluate the trained model.

We evaluate the error rate for testing set at the end of each epoch. table 3 shows the best error rate (top-1 and top-5) evaluated on testing set and adversarial examples. The later is created by Fast Gradient Sign Method (FGSM) [30],

Method / Data evaluation	Testing set		Adversarial examples	
	Top-1	Top-5	Top-1	Top-5
ERM	33.84	12.46		
Mix-up [9]	32.13	11.35	76.79	50.76
Mix-up Attack (1) ($\xi = 0.1 \rightarrow 0.01$)	32.57	10.98	65.60	37.57
Mix-up Attack (2) ($\xi = 0.01$)	31.35	10.81	71.31	44.5
Cut-Mix [10]	30.94	10.41	81.24	58.72

Table 3: : ImageNet error rate (top-1 and top-5 in %) on testing set and on adversarial examples on different training modes : ERM, Mix-Up, Mix-Up Attack and Cut-Mix.

on the trained model by ERM, with $\epsilon = 0.05$. In Mix-up Attack, n_iters is fixed at 1 and ξ is set up following two configurations, (1) ξ is reduced linearly from 0.1 to 0.01 and (2) ξ is fixed at 0.01. Following the original article, α is set at 0.2 for Mix-Up and Mix-up Attack and $\alpha = 1$ for Cut-Mix. More details for hyper-parameters can be found in section 6.

First, in Mix-up Attack (1) and (2), we see clearly the trade-off between error rate for testing set and error rate for adversarial examples. If ξ takes a large value as in (1), the error rate for testing sample can be even worse than Mix-up (without using attack stage) about 0.5%, but it gains more than 10% for the robustness against adversarial examples. On the other hand, if ξ takes a smaller value as in (2), error rates for both testing sample and adversarial examples are better than ones in Mix-Up, but it gains only about 5% for the robustness against adversarial examples. Second, Mix-up Attack (2) provides a worse error rate than Cut-Mix, about 0.4 % in the case of testing sample, but it gains about 10% in the case of adversarial examples. Therefore, we conclude that manifold attack not only improves accuracy rate on testing set but also provide significantly robustness to model against adversarial examples.

Note that, in attack stage, the model $g()$ need to be continuous. In the case of using neural network model with *Dropout* layer, the active connections need to be fixed in an attack stage to guarantee that $g()$ is continuous.

5.3 Semi-supervised manifold attack

In this subsection, we propose *semi-supervised manifold attack*, created by combining a supervised learning loss with manifold attack loss. We denote and recall:

- $f()$ the model complete, which outputs the class probability and $g()$ a part of $f()$ from the input to an intermediate layer, which outputs embedded or latent representation.
- $\mathbf{x}^l, \mathbf{x}^u$ a labelled sample and an unlabelled sample, respectively.
- N_l the number of labelled samples and N_u number of unlabelled samples, hence $N = N_u + N_l$.
- M the number of sets of anchor points, which is also number of virtual points.
- $\mathcal{B} = \{g(\mathbf{x}_1), \dots, g(\mathbf{x}_N)\} \cap \{g(\tilde{\mathbf{x}}_1), \dots, g(\tilde{\mathbf{x}}_M)\}$ set that contains all embedded representation of data samples and virtual points.

The objective function for *semi supervised manifold attack* is defined as follows :

$$L = L_s + \lambda L_u = \frac{1}{N_l} \sum_{i=1}^{N_l} \mathcal{L}_c(f(\mathbf{x}_i^l), y_i) + \lambda \frac{1}{|\mathcal{B}|} \sum_{\mathbf{a}_i \in \mathcal{B}} \mathcal{L}_e(\mathbf{a}_i, \mathcal{B} \setminus \{\mathbf{a}_i\}) \quad (4)$$

In the case if \mathcal{B} contains only embedded representation of data samples, we have the objective function for semi supervised embedding as described in [35]. The supervised loss is the ERM problem by default, but it can be Mix-up loss. The objective function eq. (4) is optimized alternatively between attack stage (γ as variable) and model update stage (model parameters as variable).

In this experiment, we convert Mix Match [36], a semi-supervised learning method, into its attack version. The explicit form of L_s and L_u can be found in the Mix Match original paper. As in Mix-up Attack, in a training batch, we add an attack stage after the sampling of γ to get Mix Match Attack. Note that, γ_1 in Mix Match differs from the Mix-up as :

$$\gamma_1 + \gamma_2 = 1, \gamma_1 \sim \text{Beta}(\alpha, \alpha) \text{ and } \gamma_1 \geq \gamma_2$$

Data	Method / Test	1	2	3	4	Mean
CIFAR-10	Mix Match	10.62	12.72	12.02	15.26	12.65 \pm 1.68
CIFAR-10	Mix Match Attack	8.84	10.46	10.09	12.89	10.57 \pm 1.47
SVHN	Mix Match	6.0925	6.73	7.802	7.37	7.0 \pm 0.65
SVHN	Mix Match Attack	5.07	5.93	5.42	5.47	5.47 \pm 0.3

Table 4: : CIFAR-10 and SVHN Error rate in four different initialization. The number of labelled sample is fixed at 250, with Wide ResNet-28 model.

Then the projection for γ_1 is now the clamping function between 0.5 and 1. In case of using separately two variables γ_1 and γ_2 , we can use the projection Π'_{ps} (3) in section 4. We reuse the implementation for Mix Match in *Pytorch* by Yui [37] (with all hyper-parameters by default), then we add the attack stage, with the number of iterations $n_{iters} = 1$. In each experiment, for both CIFAR-10 and SVHN dataset, we divide the training set into three parts : labelled set, unlabelled set and validation set. The number of validation samples is fixed at 5000, the number of labelled samples is 250, and the resting samples is for unlabelled set. We repeat the experiment four times, with different samplings of labelled samples, unlabelled samples, validation samples and different initialization of model Wide ResNet-28 [38] (about 1.47M trainable parameters). More details for hyper-parameters can be found in section 6.

The error rate on testing set, which corresponds to the best validation error rate, is reported in table 4, for both Mix Match and Mix Match Attack. We see that Mix Match Attack improves the performance of Mix Match, about 1.5% less on error rate. There is a difference between the error rate of Mix Match reproduced by our experiment and the one reported from the original paper, which probably comes from the sampling of samples, the initialization of model, the library used (*Pytorch* vs *TensorFlow*) and the way to report error rate (error rate associated to best validation error vs the median error rate of the last 20 checkpoints). Note that, there are also other semi-supervised methods in Mix-up family as : Real Mix [39], Re Mix Match [40] and we can also convert them to get their attack version, which is expected to give a better performance.

The drawback of manifold attack, first, is the additional complexity on training stage to find the adversarial γ . Therefore, n_{iter} need to be small. The second one is that virtual points or attack points can be out of the manifold of data, therefore we can have a worse result than no using manifold attack. A technical note for manifold learning can be found in section 6.

6 Conclusions

We have presented an “add-on” which can be easily integrated with the main objective function to create a Virtual Adversarial Training process, by using the linear combination of data samples. Despite the simplicity, we found that, through experiments, by using attack points as supplement data points in manifold learning, we gain a better performance on the evaluation loss. Moreover, in classification, by converting an approach in the Mix family into its attack version, we not only reduce significantly the error rate, but also gain significantly the robustness against adversarial examples. Our future work will focus on *semi supervised manifold attack* (Equation 4).

References

- [1] Yann Lecun, Yoshua Bengio, and Geoffrey Hinton. Deep learning. *Nature Cell Biology*, 521(7553):436–444, may 2015.
- [2] K Fukushima. Neocognitron: a self organizing neural network model for a mechanism of pattern recognition unaffected by shift in position. *Biological cybernetics*, 36(4):193–202, 1980.
- [3] Y. Lecun, L. Bottou, Y. Bengio, and P. Haffner. Gradient-based learning applied to document recognition. *Proceedings of the IEEE*, 86(11):2278–2324, 1998.
- [4] Alex Krizhevsky, Ilya Sutskever, and Geoffrey E Hinton. Imagenet classification with deep convolutional neural networks. In F. Pereira, C. J. C. Burges, L. Bottou, and K. Q. Weinberger, editors, *Advances in Neural Information Processing Systems 25*, pages 1097–1105. Curran Associates, Inc., 2012.
- [5] Karen Simonyan and Andrew Zisserman. Very deep convolutional networks for large-scale image recognition, 2014.
- [6] Kaiming He, Xiangyu Zhang, Shaoqing Ren, and Jian Sun. Deep residual learning for image recognition. *CoRR*, abs/1512.03385, 2015.
- [7] Christian Szegedy, Wei Liu, Yangqing Jia, Pierre Sermanet, Scott E. Reed, Dragomir Anguelov, Dumitru Erhan, Vincent Vanhoucke, and Andrew Rabinovich. Going deeper with convolutions. *CoRR*, abs/1409.4842, 2014.
- [8] G. Hinton, L. Deng, D. Yu, G. E. Dahl, A. Mohamed, N. Jaitly, A. Senior, V. Vanhoucke, P. Nguyen, T. N. Sainath, and B. Kingsbury. Deep neural networks for acoustic modeling in speech recognition: The shared views of four research groups. *IEEE Signal Processing Magazine*, 29(6):82–97, 2012.
- [9] Hongyi Zhang, Moustapha Cissé, Yann N. Dauphin, and David Lopez-Paz. mixup: Beyond empirical risk minimization. *CoRR*, abs/1710.09412, 2017.
- [10] Sangdoon, Dongyoon Han, Seong Joon Oh, Sanghyuk Chun, Junsuk Choe, and Youngjoon Yoo. Cutmix: Regularization strategy to train strong classifiers with localizable features. *CoRR*, abs/1905.04899, 2019.
- [11] Nitish Srivastava, Geoffrey Hinton, Alex Krizhevsky, Ilya Sutskever, and Ruslan Salakhutdinov. Dropout: A simple way to prevent neural networks from overfitting. *Journal of Machine Learning Research*, 15(56):1929–1958, 2014.
- [12] Golnaz Ghiasi, Tsung-Yi Lin, and Quoc V. Le. Dropblock: A regularization method for convolutional networks. *CoRR*, abs/1810.12890, 2018.
- [13] Sergey Ioffe and Christian Szegedy. Batch normalization: Accelerating deep network training by reducing internal covariate shift. *CoRR*, abs/1502.03167, 2015.
- [14] Dmitry Ulyanov, Andrea Vedaldi, and Victor S. Lempitsky. Instance normalization: The missing ingredient for fast stylization. *CoRR*, abs/1607.08022, 2016.
- [15] Jimmy Lei Ba, Jamie Ryan Kiros, and Geoffrey E. Hinton. Layer normalization, 2016.
- [16] Yuxin Wu and Kaiming He. Group normalization. *CoRR*, abs/1803.08494, 2018.
- [17] Anders Krogh and John A. Hertz. A simple weight decay can improve generalization. In J. E. Moody, S. J. Hanson, and R. P. Lippmann, editors, *Advances in Neural Information Processing Systems 4*, pages 950–957. Morgan-Kaufmann, 1992.
- [18] Carl Doersch, Abhinav Gupta, and Alexei A. Efros. Unsupervised visual representation learning by context prediction, 2015.
- [19] N. Morgan and H. Bourlard. Generalization and parameter estimation in feedforward nets: Some experiments. In D. S. Touretzky, editor, *Advances in Neural Information Processing Systems 2*, pages 630–637. Morgan-Kaufmann, 1990.
- [20] Lutz Prechelt. Automatic early stopping using cross validation: Quantifying the criteria. *Neural Networks*, 11:761–767, 1997.
- [21] Diederik P. Kingma and Jimmy Ba. Adam: A method for stochastic optimization, 2014.
- [22] Ilya Loshchilov and Frank Hutter. SGDR: stochastic gradient descent with restarts. *CoRR*, abs/1608.03983, 2016.
- [23] Jan Kukacka, Vladimir Golkov, and Daniel Cremers. Regularization for deep learning: A taxonomy. *CoRR*, abs/1710.10686, 2017.
- [24] Chiyuan Zhang, Samy Bengio, Moritz Hardt, Benjamin Recht, and Oriol Vinyals. Understanding deep learning requires rethinking generalization. *CoRR*, abs/1611.03530, 2016.

- [25] Takeru Miyato, Shin ichi Maeda, Masanori Koyama, and Shin Ishii. Virtual adversarial training: A regularization method for supervised and semi-supervised learning, 2017.
- [26] J.B. Kruskal and M. Wish. *Multidimensional Scaling*. Sage Publications, 1978.
- [27] Mikhail Belkin and Partha Niyogi. Laplacian eigenmaps for dimensionality reduction and data representation. *Neural Computation*, 15:1373–1396, 2003.
- [28] Sam T. Roweis and Lawrence K. Saul. Nonlinear dimensionality reduction by locally linear embedding. *SCIENCE*, 290:2323–2326, 2000.
- [29] Geoffrey Hinton and Sam Roweis. Stochastic neighbor embedding. *Advances in neural information processing systems*, 15:833–840, 2003.
- [30] Ian J. Goodfellow, Jonathon Shlens, and Christian Szegedy. Explaining and harnessing adversarial examples, 2014.
- [31] J. Deng, W. Dong, R. Socher, L.-J. Li, K. Li, and L. Fei-Fei. ImageNet: A Large-Scale Hierarchical Image Database. In *CVPR09*, 2009.
- [32] Alex Krizhevsky, Vinod Nair, and Geoffrey Hinton. Learning multiple layers of features from tiny images. *Technical report, University of Toronto*, 2009.
- [33] Yuval Netzer, Tao Wang, Adam Coates, Alessandro Bissacco, Bo Wu, and Andrew Y. Ng. Reading digits in natural images with unsupervised feature learning. *NIPS Workshop on Deep Learning and Unsupervised Feature Learning*, 2011.
- [34] Martins Frolovs. *ImageNet-Datasets-Downloader*, 2019.
- [35] Jason Weston and Frédéric Ratle. Deep learning via semi-supervised embedding. In *International Conference on Machine Learning*, 2008.
- [36] David Berthelot, Nicholas Carlini, Ian Goodfellow, Nicolas Papernot, Avital Oliver, and Colin Raffel. Mixmatch: A holistic approach to semi-supervised learning, 2019.
- [37] Yui. *Pytorch Implementation for Mix Match*, 2019. imikushana@gmail.com.
- [38] Sergey Zagoruyko and Nikos Komodakis. Wide residual networks, 2016.
- [39] Varun Nair, Javier Fuentes Alonso, and Tony Beltramelli. Realmix: Towards realistic semi-supervised deep learning algorithms, 2019.
- [40] David Berthelot, Nicholas Carlini, Ekin D. Cubuk, Alex Kurakin, Kihyuk Sohn, Han Zhang, and Colin Raffel. Remixmatch: Semi-supervised learning with distribution alignment and augmentation anchoring, 2019.

Appendix

Projection for sum and positive

Proof, by using Lagrange multiplier, problem 2 becomes:

$$\min_{\gamma, \mu \in \mathbb{R}^p, \lambda} \frac{1}{2} \sum_{i=1}^p \|\kappa_i - \gamma_i\|_2^2 + \lambda \left(\sum_{i=1}^p \gamma_i - c \right) + \sum_{i=1}^p \mu_i \gamma_i$$

subject to : $\mu_1, \mu_2, \dots, \mu_p \leq 0$

We solve the following system of equations:

$$\begin{cases} \gamma_i - \kappa_i + \lambda + \mu_i = 0 \\ \sum_{i=1}^p \gamma_i = c \\ \mu_i \gamma_i = 0 \\ \mu_i \leq 0 \\ \gamma_i \geq 0 \end{cases} \Leftrightarrow \begin{cases} \lambda = \frac{1}{p} (\sum_{i=1}^p \kappa_i - \sum_{i=1}^p \mu_i - c) \\ \gamma_i = \kappa_i - \frac{1}{p} (\sum_{i=1}^p \kappa_i - c) - \frac{p-1}{p} \mu_i + \frac{1}{p} \sum_{j \neq i} \mu_j \\ \sum_{i=1}^p \gamma_i = c \\ \mu_i \gamma_i = 0 \\ \mu_i \leq 0 \\ \gamma_i \geq 0 \end{cases}$$

If $\kappa_i - \frac{1}{p} (\sum_{i=1}^p \kappa_i - c) < 0$, we infer that $\mu_i \neq 0$ (because if $\mu_i = 0$ then $\gamma_i < 0$). From $\mu_i \neq 0$, we infer that $\gamma_i = 0$.

Let $\mathcal{P} = \{i | \kappa_i - \frac{1}{p} (\sum_{i=1}^p \kappa_i - c) > 0\}$ and $\mathcal{N} = \{i | \kappa_i - \frac{1}{p} (\sum_{i=1}^p \kappa_i - c) < 0\}$. We find exactly the same problem as before, but with only active index in the set \mathcal{P} .

$$\begin{cases} \gamma_i - \kappa_i + \lambda + \mu_i = 0, \forall i \in \mathcal{P} \\ \sum_{i \in \mathcal{P}} \gamma_i = c \\ \mu_i \gamma_i = 0, \forall i \in \mathcal{P} \\ \mu_i \leq 0, \forall i \in \mathcal{P} \\ \gamma_i \geq 0, \forall i \in \mathcal{P} \end{cases}$$

Then we repeat until the constraint satisfaction for γ . Here is an implementation for multiple κ ($\kappa \in \mathbb{R}^{M \times P}$) in *pytorch*.

```
def prox_positive_and_sum_constraint(x, c):
    """ x is 2-dimensional array (M \times p) """

    n = x.size()[1]
    k = (c - torch.sum(x, dim=1))/float(n)
    x_0 = x + k[:, None]
    while len(torch.where(x_0 < 0)[0]) != 0:
        idx_negative = torch.where(x_0 < 0)
        x_0[idx_negative] = 0.

        one = x_0 > 0
        n_0 = one.sum(dim=1)
        k_0 = (c - torch.sum(x_0, dim=1))/n_0
        x_0 = x_0 + k_0[:, None] * one

    return x_0
```

Manifold attack for embedded representation

Architecture of model $g()$ (*Pytorch* style) used in section 5.1 :

- S curve data : $Conv1d[1, 4, 2] \rightarrow ReLu \rightarrow Conv1d[4, 4, 2] \rightarrow ReLu \rightarrow Flatten \rightarrow Fc[4, 2]$.
- Digit data : $Conv2d[1, 8, 3] \rightarrow ReLu \rightarrow Conv2d[8, 16, 3] \rightarrow ReLu \rightarrow Flatten \rightarrow Fc[64, 2]$.

Optimizer : Stochastic gradient descent, with learning rate $lr = 0.001$ and momentum = 0.9. Learning rate is reduce by $lr = lr^{0.5}$ after each 10 epochs. The number of epochs is 40.

MultiDimensional Scaling

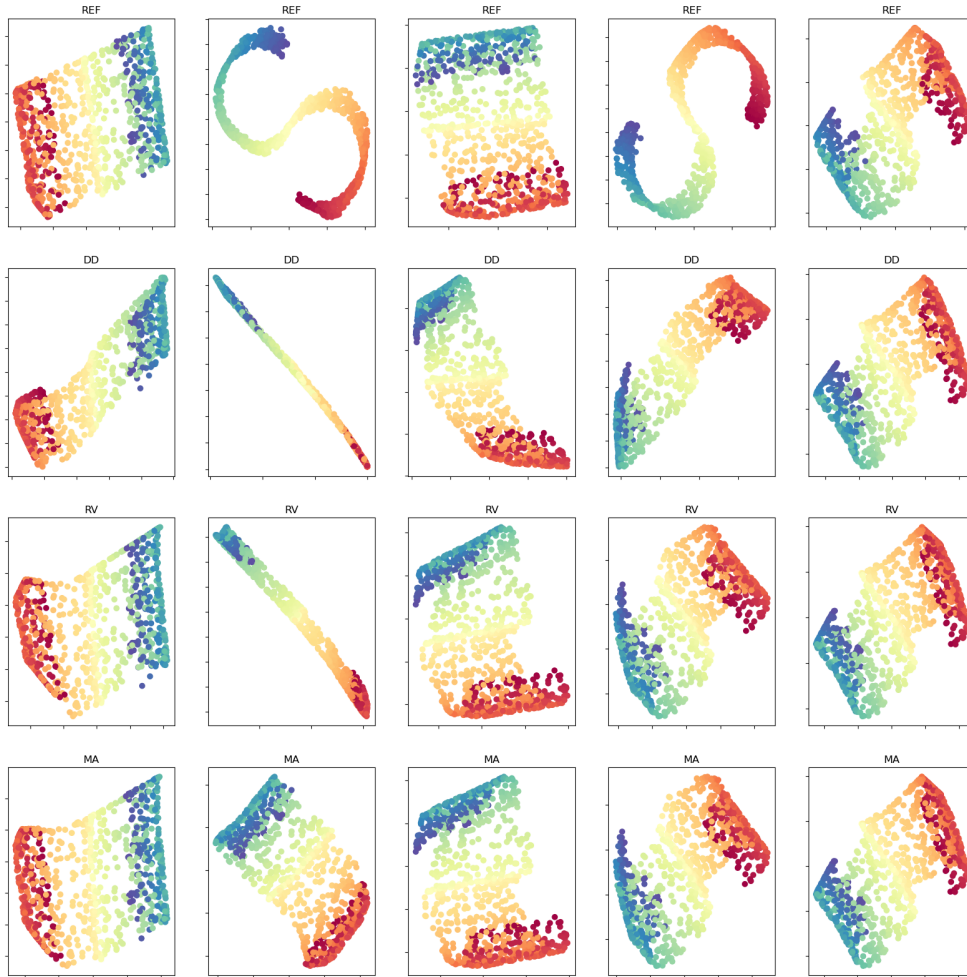


Figure 3: Five evaluations with different initialization of model for the S curve data, using manifold learning method MDS with four modes : REF, DD, RV (NA), MA (NA). We see clearly the effect of Manifold Attack by the second column. Thus, the embedded representation of Manifold Attack is more spread compared to Random Virtual.

Robustness to adversarial examples

Hyper-parameters : optimizer = Stochastic gradient descent, number of epochs = 300, learning rate = 0.1, momentum = 0.9, learning rate is reduce by $lr = 0.1lr$ after each 75 epochs, batch size = 200, weight decay = 0.0001.

Laplacian eigenmaps

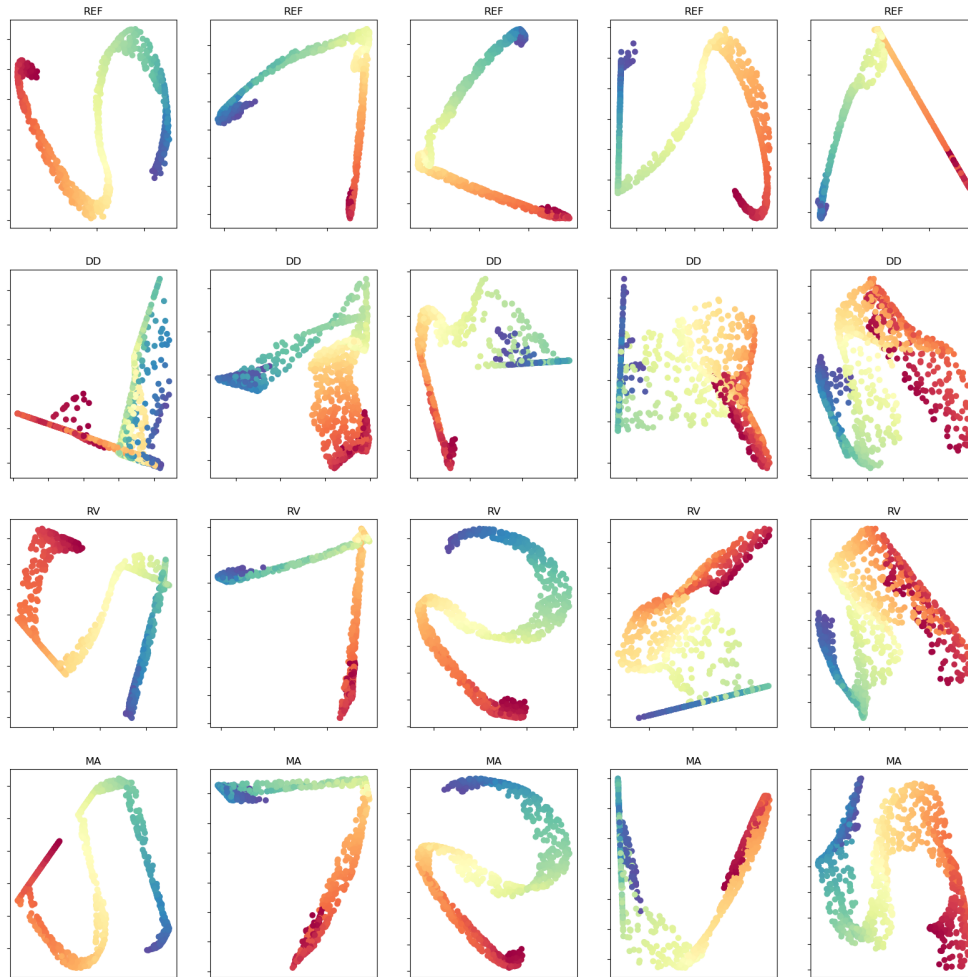


Figure 4: Five evaluations with different initialization of model for the S curve data, using manifold learning method LE with four modes : REF, DD, RV (NA), MA (NA). We see clearly the effect of Manifold Attack by the fourth column, where the embedded representation shape of Manifold Attack is more similar to Reference than one of Random Virtual.

Semi-supervised manifold attack

Hyper-parameters : optimizer = Adam, number of epochs = 1024, learning rate = 0.002, $\alpha = 0.75$, batch size labelled = batch size unlabelled = 64, T = 0.5 (in sharpening), $\lambda = 75$ (linearly ramp up from 0), EMA = 0.999 , error validation after 1024 batches.

To reproduce an experiment, we define function `seed_` as:

```
def seed_(p):
    """ for reproducible """
    torch.manual_seed(p)
    np.random.seed(p)
```



```

random.seed(p)
if torch.cuda.is_available():
    torch.cuda.manual_seed(p)
torch.backends.cudnn.deterministic = True
torch.backends.cudnn.benchmark = False

return 0

```

The four experiment 1,2,3,4 in table 4 are launched with respectively seed_(0), seed_(1), seed_(2), seed_(3).

In Mix-up Attack, n_iters is fixed at 1. In dataset CIFAR-10, ξ starts at 0.1 and decreases linearly to 0.01 after 1024 epochs. In dataset SVHN, ξ starts at 0.1 and decreases linearly to 0.01 after 1024 epochs for seed_(0) and seed_(3); ξ starts at 0.1 and decreases linearly to 0.001 after 1024 epochs for seed_(2); ξ starts at 0.01 and decreases linearly to 0.001 after 1024 epochs for seed_(1)

Technical notes

By using manifold learning, we analyse the supplement complexity via two factors : the gpu memory and the execution time.

gpu memory : Denote M number of virtual points in a batch and p is the number of anchor points in a set, normally in the attack stage, we need to reserve the memory for $N_b \times p$ samples. Maybe this is not a problem for datasets as CIFAR-10 or SVHN (which has small size for a sample, about $32 \times 32 \times 3$ pixels), but for large dataset as ImageNet, each sample has about $224 \times 224 \times 3$ pixels after cropping, this can make the run out of memory in gpu. A solution is to use a system of index that connect (each time) p anchor points in a batch. Let consider the following problem for calculating the gradient backward in attack stage, to update the coefficient γ :

$$\nabla_{\gamma} \mathcal{L}_t(\{\gamma_1^k \mathbf{z}_1^k + \gamma_2^k \mathbf{z}_2^k + \dots + \gamma_p^k \mathbf{z}_p^k | k = 1, \dots, M\})$$

Then the memory needed to reserve anchor points is equivalent to $M \times p$ samples. If anchor points are sampled from data samples, we denote :

- $\mathbf{X}^b \in \mathbb{R}^{N_b \times K \times H \times W}$, input batch (images), where N_b is number of inputs in a batch, K, H, W are respectively number of channel, height and width.
- $\mathbf{M} \in \mathbb{R}^{N_b \times M}$, index matrix (or mask matrix) for M sets of anchor points. $\mathbf{M}[i, k] = \begin{cases} 1 & \text{if sample } i \text{ of } \mathbf{X}^b \text{ is an anchor point in set } k, \\ 0 & \text{otherwise.} \end{cases}$
- $\Gamma \in \mathbb{R}^{N_b \times M}$, coefficients associated to each input (in a column), and M is the number of sets of anchor points. Γ is initialized as follows : $\Gamma = \mathbf{0}_{N_b \times M}$, $\Gamma[\mathbf{M}[:, k], k] = \gamma^k, k = 1, \dots, M$.

The system of index for anchor points is performed by *einsum* function and by a mask matrix \mathbf{M} . Then all virtual points are inferred by :

$$\text{einsum}("N_b K H W, N_b M \rightarrow M K H W", \mathbf{X}^b, \Gamma)$$

Then we update Γ by the corresponding gradient by mask matrix \mathbf{M} :

$$\begin{aligned} \Gamma &\leftarrow \Gamma + \nabla_{\Gamma} \mathcal{L}_t(\Gamma) \circ \mathbf{M} \\ \Gamma[\mathbf{M}[:, k], k] &\leftarrow \Pi_{ps}(\Gamma[\mathbf{M}[:, k], k]), k = 1, \dots, M \end{aligned}$$

In short, by using *einsum* function, the memory needed is reduced from $M \times p$ samples equivalent to N_b samples equivalent (two supplement matrices $\Gamma, \mathbf{M} \in \mathbb{R}^{N_b \times M}$ are negligible compared to N_b samples equivalent). Not that, usually M is approximated to N_b then, we reduce p times the memory needed.

execution time : In a batch training (no attack), execution time can be decomposed into : *loading batch data time* (pre-processing included) and *working time* (loss calculating + gradient back propagation + model updating time). When adding attack stage, via our experiments, the execution time becomes: *loading batch data time* + *working time* $\times n_iters$, with hypothesis that time for gradient back propagation is the most essential in *working time*. Therefore, n_iters must take a small value.